

PACS numbers: 82.37.Vb; 78.35.+c; 78.67.Ch; 82.65.+r
DOI: 10.1070/QE2009v039n07ABEH014022

Four-photon microwave laser spectroscopy of molecules in the hydration layers of biopolymers and nanoparticles

A.F. Bunkin, S.M. Pershin

***Abstract*. Four-photon laser scattering spectra of bidistilled water and aqueous solutions of biopolymers (proteins and DNA), carbon nanotubes and hydrogen peroxide have been measured in the range ± 10 cm^{-1}. The spectra show rotational resonances of H_2O_2, ortho-H_2O and para-H_2O molecules. The resonance contribution of the H_2O rotational spectrum to the four-photon scattering signal in the solutions of the biopolymers and hydrophobic nanoparticles is an order of magnitude larger in comparison with water, which points to free rotation of the water molecules near the surface of such particles. This effect is due to the formation of water depletion layers near hydrophobic nanoparticles, as predicted in earlier theoretical studies.**

Keywords: *nonlinear laser spectroscopy, four-wave mixing, low-frequency spectroscopy of biopolymers, hydration of macromolecules.*

1. Introduction

Recent advances in bio- and nanotechnologies have led many researchers to focus on the study of interfacial layers between water and biomolecules, water and hydrophilic/hydrophobic nanoparticles, and water and micro- or nanocapillaries [1 – 5]. The physical state of water in a hydration shell depends significantly on the nature of the interaction between the H_2O molecules and the nanoparticle being hydrated. In particular, Stillinger [6] assumed as early as 1973 that, at a water – hydrophobe interface, there is a layer with a density substantially lower than that of bulk water at a distance of the order of 1 – 1.5 nm (three to five H_2O molecules) from the interface. This idea was elaborated in later theoretical studies [1, 2, 7] and has recently been confirmed in experimental studies of X-ray scattering from interfaces between water and monomolecular layers of hydrophobic polymers [8, 9] and in measurements of the thermal conductance of interfacial layers between water and hydrophobic nanoparticles [10].

There is now ample experimental evidence that hydrophilic biomolecules, in particular, many proteins, are capable of structuring water molecules in the hydration layer, producing structures similar to hexagonal or cubic ice at room temperature [11 – 13]. Such behaviour is exhibited, e.g., by insect cuticle proteins [11, 12]. For this reason, insects easily withstand multiple freeze – thaw cycles: the water in their cuticle has the hexagonal ice structure at room temperature [11]. Most studies in this field employed X-ray scattering [11, 12] or slow-neutron scattering. In a number of works, terahertz spectroscopy was utilised to probe the hydration shells of hydrophilic biomolecules in thin water films [13, 14].

The principal difficulty in studies of the hydration layers of biomolecules and nanoparticles by optical spectroscopy is that such layers contain a relatively small number of molecules, but their signal should be separated from the background produced by the water molecules located outside the layer. Therefore, a sufficiently sensitive (large signal-to-noise ratio), nondestructive method is needed, which would enable measurements in the region where the optical spectrum of the system is most strongly dependent on intermolecular interactions. In the case of water, this is the range from several to ~ 200 cm^{-1}, which includes translational (~ 180 cm^{-1}) and transverse (~ 60 cm^{-1}) intermolecular vibrational modes.

Spectroscopic studies in this range are, however, difficult to perform, primarily because there are at present no effective, widely tunable microwave sources for terahertz spectroscopy. Moreover, the use of spontaneous Raman scattering is limited by the weak intensity of intermolecular resonances [15] and the high background level near the excitation line as a result of the elastic scattering of the probe laser beam. Yet another impediment to the use of IR spectroscopy is uncontrolled heating of the sample and the necessity to use thin layers of aqueous solutions, so that the influence of the cell wall cannot be precluded.

Our group was the first to utilise four-wave mixing (FWM) spectroscopy to overcome these difficulties [16 – 19], which enabled us to substantially reduce the low-frequency signal-to-noise ratio by phasing molecular motions in a microscopic volume using two laser beams at frequencies ω_1 and ω_2, with the frequency difference $\omega_1 - \omega_2$ varied in a wide spectral region, from the far-IR to the centimetre range. In this technique, the parameter to be measured is the intensity of the radiation of frequency $\omega_s = \omega_1 - (\omega_1 - \omega_2)$ passed through a polarisation analyser crossed with the polarisation of the $\boldsymbol{E}^{(2)}$ wave. The nonlinear polarisation of this radiation is given by [20]

$$\boldsymbol{P}_i^{(3)} = 6\chi_{ijkl}^{(3)}(\omega_s, \omega_1, \omega_2, -\omega_1)\boldsymbol{E}_j^{(1)}\boldsymbol{E}_k^{(2)}\boldsymbol{E}_l^{(1)*}. \quad (1)$$

A.F. Bunkin, S.M. Pershin A.M. Prokhorov General Physics Institute, Russian Academy of Sciences, ul. Vavilova 38, 119991 Moscow, Russia; e-mail: abunkin@orc.ru, pershin@orc.ru

Received 12 December 2008; revision received 28 January 2009
Kvantovaya Elektronika **39** (7) 638 – 642 (2009)
Translated by O.M. Tsarev

Here, $\chi^{(3)}$ is the third-order susceptibility; $\boldsymbol{E}^{(1)}$ and $\boldsymbol{E}^{(2)}$ are the amplitudes of the interacting fields; and $I_s \propto |\chi^{(3)}|^2 I_1^2 I_2$ is the measured signal intensity. When the difference $\omega_1 - \omega_2$ is tuned to the frequency of a vibrational or rotational molecular resonance, the transition produces an ensemble of coherent states, which can be described by collective quantum-mechanical variables [21].

Another important issue in the physics of liquids, in particular, in the physics of water, is a detailed understanding of hydrogen bonding in media where the molecules differ in the nuclear spin of their hydrogen atoms. One example of such molecules is the ortho and para forms (spin isomers) of water, in which the total spin of the hydrogen atoms is either unity (ortho molecules) or zero (para molecules). Under equilibrium conditions, the ortho to para ratio is 3 : 1. The ortho and para molecules have different rotational spectra [22] and are easy to identify in the gas phase [23]. As shown by Tikhonov and Volkov [23], passing water vapour through a porous material with a large specific surface leads to ortho-water enrichment in the vapour. Moreover, the spin isomers differ in the rate of adsorption on the surfaces of organic (DNA, lysozyme protein) and inorganic compounds [24].

The likely reason for the selective binding of the spin isomers is that the constantly rotating ortho water molecules are more mobile, whereas the para molecules, which have a nonrotational ground state, have a greater tendency to form complexes. Comparison of the rotational spectra ($70-90$ cm^{-1}) of ortho and para H_2O molecules in distilled water and in aqueous solutions of native and denaturated DNA and protein molecules points to selective interaction between these biomolecules and para H_2O in the liquid phase [25, 26].

The objective of this work was to measure and analyse the FWM spectra of aqueous DNA and protein solutions and single-wall carbon nanotube (SWNT) suspensions in the range ± 10 cm^{-1}, the most difficult to study by optical and microwave spectroscopies. Most effort was focused on identification of the rotational lines of the H_2O molecule and its spin isomers (ortho and para molecules) in the spectra and distinctions between the low-frequency spectra of hydrophobic and hydrophilic impurities.

2. Experimental

In our experiments, we used a setup described elsewhere [27]. Two counterpropagating waves, $\boldsymbol{E}^{(1)}$ and $\boldsymbol{E}^{(2)}$, with frequencies ω_1 and ω_2 were passed through a cell containing the liquid to be studied. The entrance and exit windows of the cell were of fused quartz and had a low depolarisation level for the laser radiation used. The $\boldsymbol{E}^{(1)}$ wave (frequency-doubled Nd : YAG laser operated in a single longitudinal mode) was circularly polarised, and the frequency-tunable wave $\boldsymbol{E}^{(2)}$ was linearly polarised. With these polarisations of the coupled waves, the signal, determined by nonlinearity (1), was free of the nonresonant contribution from the electronic subsystem of the medium [20].

Since the polarisation unit vectors of the ω_s signal and $\boldsymbol{E}^{(2)}$ wave were noncollinear, whereas their propagation directions coincided, the FWM signal was separated by a Glan prism. The width of the spectrometer instrumental function (~ 0.12 cm^{-1}) and the spectral range of measurements (-1200 to 300 cm^{-1}) were determined by the output characteristics of the dye laser, which was pumped with the Nd : YAG third harmonic and ensured programmed frequency tuning of the $\boldsymbol{E}^{(2)}$ wave. For each value of ω_2, the signal was averaged over 10 to 30 repeated measurements. The laser frequency was varied automatically in ~ 0.119-cm^{-1} steps. The frequency zero was adjusted with an accuracy of 0.02 cm^{-1} using Brillouin resonances. Subsequent wavelength tuning was checked using modes of a Fabry–Perot interferometer with a 7-mm base. The uncertainty in the amplitude of the FWM signal was set by a program and was within 10 %. The uncertainty in the resonance frequency measurements was determined by the width of the spectrometer instrumental function (0.12 cm^{-1}).

Measurements were made in bidistilled water, aqueous solutions of α-chymotrypsin (10 mg mL^{-1}) and DNA (15 mg mL^{-1}), 5% aqueous hydrogen peroxide (H_2O_2) and an aqueous suspension of SWNTs (concentration below 0.1 μg mL^{-1}, corresponding to less than 10^9 nanotubes in the probed volume according to a rough estimate). The FWM signal emerged in a 5-mm-long region at the intersection of the pump beams. The liquids to be studied were not degassed.

3. Experimental results

We measured FWM spectra of an aqueous nanotube suspension and aqueous solutions of α-chymotrypsin, DNA and hydrogen peroxide in the range ± 10 cm^{-1}.

Figure 1a shows the FWM spectra of bidistilled water, the nanotube suspension and 5 % aqueous hydrogen peroxide measured under similar experimental conditions. Each data point was obtained using 30 laser shots at ~ 0.12-cm^{-1} intervals. Also shown in Fig. 1a is the FWM spectrum calculated as described previously [18].

In Fig. 1a, the numbers 1 and 5 mark the Raman resonances $(6_{16} - 5_{23})$ (0.74 cm^{-1}) and $(4_{14} - 3_{21})$ (2.26 cm^{-1}) of ortho-H_2O; 8 and 9 mark the Raman resonances $(4_{40} - 5_{33})$ (3.21 cm^{-1}) and $(2_{20} - 3_{13})$ (4.0 cm^{-1}) of para-H_2O; and 2, 3, 4, 6, 7, 10 and 11 mark the Raman lines $(2_{11} - 1_{01})$ (1.25 cm^{-1}), $(8_{27} - 9_{19})$ (1.47 cm^{-1}), $(10_{19} - 9_{27})$ (1.8 cm^{-1}), $(7_{07} - 7_{17})$ (2.75 cm^{-1}), $(9_{09} - 9_{19})$ (3.06 cm^{-1}), $(16_{016} - 16_{116})$ (4.65 cm^{-1}) and $(4_{13} - 3_{03})$ (4.8 cm^{-1}) of H_2O_2. Here, the numbers in brackets specify the rotational quantum numbers J, K_a, K_c and the wave numbers of the corresponding Raman transitions according to Rothman et al.'s classification [22]. The best agreement between the calculated and measured spectra in Fig. 1a was obtained at 15 % H_2O_2 in the hydration layer of the aqueous nanotube suspension.

Figure 1b presents the FWM spectrum of bidistilled water (Fig. 1a) with the vertical axis expanded by a factor of ten. This spectrum also shows well-defined Raman lines that correspond to rotational transitions of the H_2O_2 and H_2O molecules and are present in the spectra in Fig. 1a. The peaks of the rotational resonances in bidistilled water are an order of magnitude weaker than those in the nanotube suspension.

It follows from the data in Fig. 1 that the spectra of the aqueous nanotube suspension, aqueous H_2O_2 and bidistilled water contain the same set of resonances, corresponding to rotational transitions of the H_2O_2 and H_2O molecules, but the addition of nanotubes (0.1 μg mL^{-1}) to water increases the FWM signal due to rotational transitions by an order of magnitude relative to bidistilled water. Comparison of

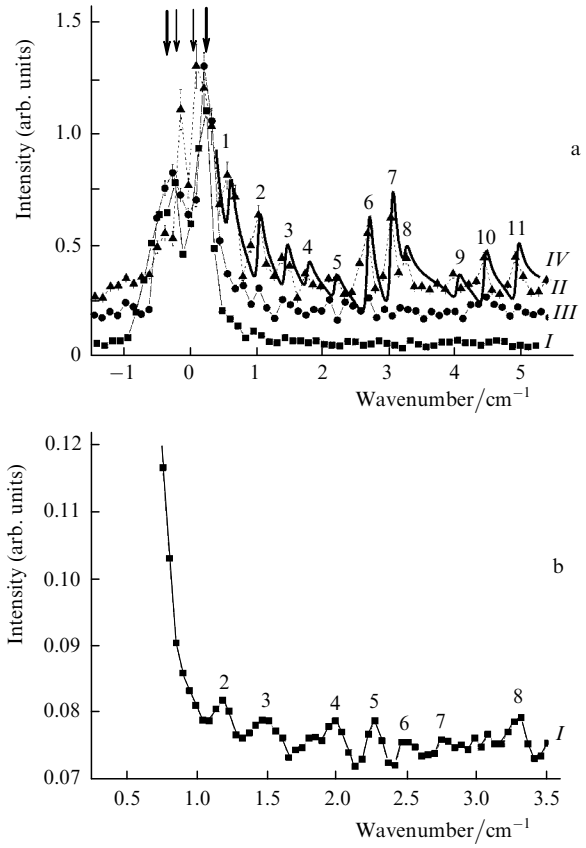

Figure 1. (a) FWM spectra of (*I*) bidistilled water, (*II*) aqueous nanotube suspension and (*III*) 5 % aqueous hydrogen peroxide; (b) FWM spectrum of bidistilled water with the vertical axis expanded by a factor of ten. Spectra *III* and *II* are offset along the vertical axis by 0.1 and 0.2 units, respectively. (*IV*) Calculated spectrum of the aqueous nanotube suspension. The thin and heavy arrows mark the positions of Brillouin resonances in the nanotube suspension and bidistilled water. (1–11) rotational Raman resonances of the H_2O and H_2O_2 molecules.

spectra *II* and *III* in Fig. 1a indicates that the contribution of H_2O_2 rotational lines to the spectrum of the aqueous nanotube suspension is considerably greater, which obviously points to the formation of hydrogen peroxide molecules at the nanotube–water interface. Note that Nakamura and Isobe [28] presented indirect evidence of hydrogen peroxide generation in aqueous fullerene suspensions, inferred from the oxidation of special reagents, but direct evidence has hitherto been lacking. Another important point is that the experimental data in Fig. 1 lends further support to the existence of a water depletion layer near the hydrophobic nanotube surface, which was predicted [1, 2, 7] and observed [8, 9] earlier. The contribution of freely rotating H_2O_2 and H_2O molecules to the FWM signal increases with the content of such molecules in the hydration layer, but most of the molecules do not contribute to the rotational spectrum because they are hydrogen-bonded to form molecular complexes.

Figure 2 shows FWM spectra of bidistilled water and an aqueous solution of α-chymotrypsin (10 mg ml^{-1}) in the range ±3 cm^{-1} (±90 GHz). Each data point was obtained using 30 laser shots at ~ 0.12-cm^{-1} intervals. The assignment of the observed lines coincides with that given above for Fig. 1.

Rotational lines of H_2O_2 molecules in FWM spectra of

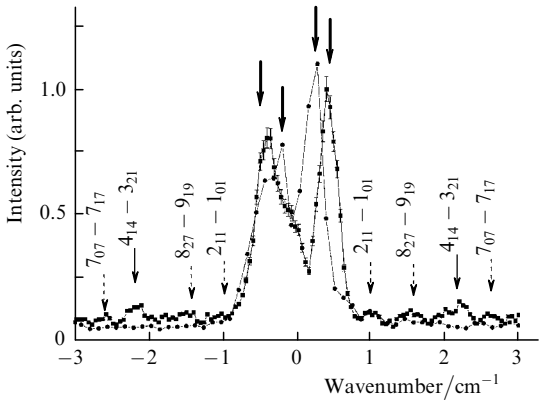

Figure 2. Portions of the FWM spectra of bidistilled water (●) and an aqueous α-chymotrypsin (10 mg mL^{-1}) solution (■). The two lines in the middle of each spectrum (marked by heavy arrows) correspond to Brillouin resonances. The thin arrows mark the position of the rotational Raman line ($4_{14}-3_{21}$) (±2.26 cm^{-1}) of ortho-H_2O, and the dashed arrows mark the positions of the rotational resonances H_2O_2 ($2_{11}-1_{01}$) (±1.25 cm^{-1}), ($8_{27}-9_{19}$) (±1.47 cm^{-1}) and ($7_{07}-7_{17}$) (±2.75 cm^{-1}).

aqueous solutions of biopolymers are also seen in Fig. 3a, which shows the spectra of an aqueous DNA solution (15 mg mL^{-1}) and bidistilled water in the range −7 to

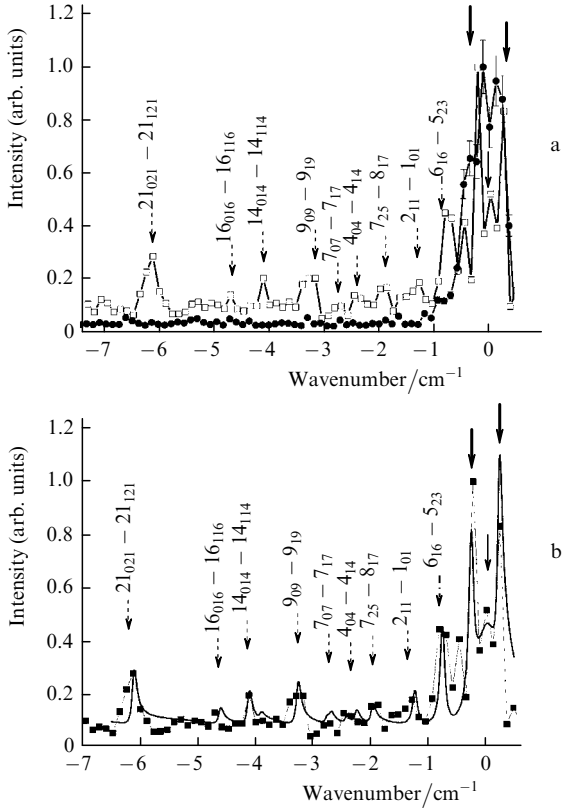

Figure 3. (a) FWM spectra of an aqueous DNA solution (□) and bidistilled water (●); (b) measured (squares) and calculated (heavy line) FWM spectra of the aqueous DNA solution (15 mg mL^{-1}). The heavy and thin arrows mark the positions of Brillouin and Rayleigh resonances, and the dashed arrows mark the positions of the Raman lines of H_2O_2: ($2_{11}-1_{01}$) (±1.25 cm^{-1}), ($7_{25}-8_{17}$) (±1.92 cm^{-1}), ($4_{04}-4_{14}$) (±2.41 cm^{-1}), ($7_{07}-7_{17}$) (±2.75 cm^{-1}), ($9_{09}-9_{19}$) (±3.06 cm^{-1}), ($14_{014}-14_{114}$) (±4.12 cm^{-1}), ($16_{016}-16_{116}$) (±4.65 cm^{-1}), ($21_{021}-21_{121}$) (± 6.16 cm^{-1}). The dot-dashed arrow marks the position of the Raman line ($6_{16}-5_{23}$) (±0.74 cm^{-1}) of ortho-H_2O.

1 cm^{-1}. Figure 3b compares the measured and calculated FWM spectra of the aqueous DNA solution.

It is clear from the FWM spectra in Fig. 3a that the DNA concentration used in our experiments increases the signal from the H_2O_2 molecules in the aqueous solution by six times, which seems to imply the corresponding increase in the hydrogen peroxide concentration in the hydration layer of the DNA.

To calculate FWM spectra of aqueous DNA solutions, we used standard formulas [20]:

$$\chi^{(3)} = \chi^{\mathrm{NR}} + \frac{\chi^{\mathrm{B}}}{(-\mathrm{i} + (\Delta \pm \Omega_{\mathrm{B}})/\Gamma_{\mathrm{ap}}} + \frac{\chi^{\mathrm{R}}}{-\mathrm{i} + \Delta/\Gamma_{\mathrm{R}}} + \\ + \sum_n \frac{\chi_n^{\mathrm{rot}}}{(-\mathrm{i} + (\Delta \pm \Omega_n)/\Gamma_{\mathrm{ap}})}, \qquad (2)$$

$$I_{\mathrm{s}} \propto |\chi^{(3)}|^2 I_1^2 I_2.$$

Here, $2\Gamma_{\mathrm{ap}}$ is the spectral resolution of our setup (0.12 cm^{-1}); Γ_{R} is the full width at half maximum of the Rayleigh wing (fitting parameter); χ_n^{rot} and Ω_n are the nonlinear optical susceptibility and centre frequency (cm^{-1}) of rotational transitions of H_2O_2 and H_2O molecules; Ω_{B} is the Brillouin resonance frequency evaluated from the FWM spectra of the aqueous DNA solution (Fig. 3); $\Delta = (\omega_1 - \omega_2)2\pi c$ is the frequency difference (cm^{-1}) (variable parameter); c is the speed of light in vacuum; χ^{B}, χ^{R} and χ^{NR} are the nonlinear third-order susceptibilities of Brillouin and Rayleigh resonances and the nonresonant susceptibility of the solution, respectively. The spectroscopic characteristics of the H_2O_2 and H_2O molecules were taken from Rothman et al. [22]. The relative concentration of H_2O_2 and H_2O molecules in the hydration layer of DNA was a fitting parameter. This procedure ensures good agreement between measured and calculated FWM spectra of aqueous DNA solutions, as illustrated in Fig. 3b.

A noteworthy feature of the measured spectra in Figs 1 and 2 is that the Brillouin resonance frequency varies markedly from solution to solution. For example, the frequency range between the Brillouin maxima is $\Delta f_{\mathrm{B}} \approx \pm 0.12$ cm^{-1} in the aqueous nanotube suspension (thin arrows in Fig. 1a), $\Delta f_{\mathrm{B}} = \pm 0.4$ cm^{-1} in the α-chymotrypsin solution and $\Delta f_{\mathrm{B}} = \pm 0.25$ cm^{-1} in bidistilled water (Fig. 2). It is known [29] that

$$\Delta f_{\mathrm{B}} = \frac{2 v_{\mathrm{s}} n \sin(\varphi/2)}{c\lambda}, \qquad (3)$$

where n is the index of refraction; λ is the probe wavelength; φ is the angle between the incident and scattered waves; and v_{s} is the ultrasound velocity in the probed medium. Under normal conditions, distilled water has $n = 1.33$, $v_{\mathrm{s}} = 1490$ m s^{-1}. Given that $\lambda = 532$ nm and $\varphi = \pi$ in our experiments, we obtain $\Delta f_{\mathrm{B}} = \pm 0.25$ cm^{-1} in bidistilled water, in perfect agreement with the experimental data in Figs 1 and 2. The reason for the deviation of Δf_{B} from ± 0.25 cm^{-1} in the protein solution and aqueous nanotube suspension in our experiments is that these liquids have a different adiabatic compressibility, because [29]

$$(v_{\mathrm{s}})^2 = (\rho K_{\mathrm{s}})^{-1}, \qquad (4)$$

where K_{s} is the adiabatic compressibility of the liquid and ρ is its density. Therefore, the observed marked difference in Δf_{B} between bidistilled water and the samples containing the protein and nanotubes can be accounted for merely by local changes in the adiabatic compressibility K_{s} of the hydration layers of the protein and nanotubes.

Note that it is not quite correct to use formulas (3) and (4) in interpreting four-photon scattering by a lattice of ultrasonic waves excited in a locally inhomogeneous medium by two laser beams, as in our experiments. The shift of the Brillouin resonances in Figs 1–3 reflects the variation in the local propagation velocity of density fluctuations in the medium consisting of biopolymers or nanotubes suspended in water, rather than in the velocity throughout the macroscopic sample. Before dying out, an excited ultrasonic wave interacts with the laser radiation, giving rise to the Brillouin resonances shown in Figs 1–3.

4. Discussion

Water is known to be a strongly associated liquid. Each water molecule is capable of forming up to four hydrogen bonds with its neighbours. At room temperature, the average coordination number of hydrogen bonds is 3.5 [15]. At the same time, our experiments demonstrate that the FWM spectra of water and aqueous solutions contain narrow resonances whose frequencies coincide to within the width of the spectrometer instrumental function with the frequencies of rotational transitions in the vibronic ground state of the H_2O molecule (Fig. 1). One can separately identify lines due to both ortho and para H_2O molecules. Note that a similar picture is observed in rovibrational spectra of H_2O molecules in liquid helium nanodroplets [30] and solid argon matrices [31], where one also observes transitions corresponding to the ortho and para forms, and their frequencies coincide with those in the gas phase to within the width of the instrumental function. In our experiments, the spectra were measured in the range ± 10 cm^{-1}, so the possible shift of the observed resonances relative to the frequencies in the gas phase [22] was of the same order as the width of the spectrometer instrumental function (~ 0.12 cm^{-1}) because even in highly polar liquids the frequency shift is typically within 1 %–2 % [32, p. 233].

The presence of rotational lines of the H_2O_2 and H_2O molecules in the observed spectra can be understood in terms of the physical properties of the water on the surface of microimpurities [33–35]. It is known [34, 35] that hydration of hydrophilic impurities leads to structuring of the water molecules in their solvation shell. This is supported by molecular dynamics simulations [34] and X-ray structure analysis results [33].

On the other hand, recent theoretical [1, 2, 36, 37] and experimental [8, 9] results point to the formation of a depletion layer near hydrophobic surfaces of macromolecules and nanoparticles in aqueous solutions, which is similar in physical properties to water vapour. This also leads to the presence of free water molecules and rotational Raman resonances in the FWM spectrum.

In the spectra of aqueous solutions of biological macromolecules (protein, DNA), the rotational lines are stronger by almost one order of magnitude, indicating that biopolymer molecules are capable of substantially increasing the effective concentration of quasi-free water molecules in the solvation shell. In addition, this suggests that the observed

rotational lines of H_2O molecules are unrelated to air bubbles that might be present in the samples.

The formation of H_2O_2 and OH molecules in the hydration layers of carbon nanotubes and biopolymers in our spectroscopic experiments is in qualitative agreement with the experimental results reported by Nakamura and Isobe [28], who observed oxidation of small amounts of phosphors in aqueous fullerene solutions.

5. Conclusions

We observed rotational resonances of H_2O_2, ortho-H_2O and para-H_2O in bidistilled water and aqueous solutions of biopolymers (proteins and DNA) and carbon nanotubes. The resonance contribution of the H_2O rotational spectrum to the FWM signal in the solutions of the biopolymers and hydrophobic nanoparticles is an order of magnitude larger in comparison with water, which points to free rotation of the water molecules near the surface of such particles. This effect is due to the formation of water depletion layers near hydrophobic nanoparticles, as predicted in earlier theoretical studies [36, 37].

Acknowledgements. This work was supported in part by the Russian Foundation for Basic Research (Grant Nos 09-02-01173 and 08-02-00008), the Russian Academy of Sciences (Optical Spectroscopy and Frequency Standards Programme) and the Federal Agency for Science and Innovations (Support to Scientific Schools Programme, Grant No. NSh-8108.2006.2).

References

1. Garde S., Hammer G., Garcia A.E., Paulaitis M.E., Pratt L.R. *Phys. Rev. Lett.*, **77**, 4966 (1996).
2. Miller T.F., Vanden-Eijnden E., Chandler D. *Proc. Natl. Acad. Sci.*, **104**, 14559 (2007).
3. Liu P., Huang X.H., Zhou R.H., Berne B.J. *Nature (London)*, **437**, 159 (2005).
4. Zhu Y., Granick S. *Phys. Rev. Lett.*, **88**, 106102 (2002).
5. Levy Y., Onuchic J.N. *Proc. Natl. Acad. Sci.*, **101**, 3325 (2004).
6. Stillinger F.H. *J. Solution Chem.*, **2**, 141 (1973).
7. Willard A.P., Chandler D. *J. Phys. Chem. B*, **112**, 6187 (2008).
8. Poynor A., Hong L., Robinson I.K., Granick S., Zhang Z., Fenter P.A. *Phys. Rev. Lett.*, **97**, 266101 (2006).
9. Mezger M., Reichert H., Schöder S., Okasinski J., Schröder H., Dosch H., Palms D., Ralston J., Honkimäki V. *Proc. Natl. Acad. Sci.*, **103**, 18401 (2006).
10. Ge Z., Cahill D.G., Braun P.V. *Phys. Rev. Lett.*, **96**, 186101 (2006).
11. Liou Y.-C., Tocilj A., Davies P.L., Jia Z. *Nature*, **406**, 322 (2000).
12. Graether S.P., Kuiper M.J., Gagne S.M., Walker V.K., Jia Z., Sykes B.D., Davies P.L. *Nature*, **406**, 325 (2000).
13. Heugen U., Schwaab G., Brundermann E., Heyden M., Yu X., Leitner D.M., Havenith M. *Proc. Natl. Acad. Sci.*, **103**, 12301 (2006).
14. Ebbinghaus S., Kim S.J., Heyden M., Yu. X., Gruebele M., Leitner D.M., Havenith M. *J. Am. Chem. Soc.*, **130**, 2374 (2008).
15. Eisenberg D., Kauzmann W. *The Structure and Properties of Water* (Oxford: Clarendon Press, 2005).
16. Bunkin A.F., Pershin S.M., Gorchakov A.P., Nurmatov A.A. *Pis'ma Zh. Tekh. Fiz.*, **32**, 20 (2006).
17. Bunkin A.F., Nurmatov A.A., Pershin S.M. *Usp. Fiz. Nauk*, **176**, 883 (2006).
18. Bunkin A.F., Pershin S.M. *J. Raman Spectrosc.*, **39**, 726 (2008).
19. Bunkin A.F., Nurmatov A.A., Pershin S.M. *Laser Phys.*, **17**, 22 (2007).
20. Akhmanov S.A., Koroteev N.I. *Metody nelineinoi optiki v spektroskopii rasseyaniya sveta* (Nonlinear Optical Methods in Light Scattering Spectroscopy) (Moscow: Nauka, 1981).
21. Andreev A.V., Emel'yanov V.I., Il'inskii Yu.A. *Cooperative Effects in Optics* (London: Taylor & Francis, 1993; Moscow: Nauka, 1988).
22. Rothman L., Jacquemart D., Barbe A., et al. *J. Quant. Spectr. Radiat. Transfer*, **96**, 139 (2005).
23. Tikhonov V.I., Volkov A.A. *Science*, **296**, 2363 (2002).
24. Potekhin S.A., Khusainova R.S. *Biophys. Chem.*, **118**, 79 (2005).
25. Bunkin A.F., Nurmatov A.A., Pershin S.M., Khusainov R.S., Potekhin S.A. *Kvantovaya Elektron.*, **37**, 941 (2007) [*Quantum Electron.*, **37**, 941 (2007)].
26. Bunkin A.F., Pershin S.M., Nurmatov A.A. *Laser Phys. Lett.*, **3**, 275 (2006).
27. Bunkin A.F., Nurmatov A.A. *Laser Phys.*, **13**, 328 (2003).
28. Nakamura E., Isobe H. *Acc. Chem. Res.*, **36**, 807 (2003).
29. Fabelinskii I.L. *Usp. Fiz. Nauk*, **37**, 821 (1994).
30. Frochtenicht R., Kalodis M., Koch M., Huisken F. *J. Chem. Phys.*, **105**, 6128 (1996).
31. Redington R.L., Milligan D.E. *J. Chem. Phys.*, **37**, 2162 (1962); Michout X., Vasserot A.-M., Abouaf-Marguin L. *Vibr. Spectrosc.*, **34**, 83 (2004).
32. Vol'kenshtein M.V., El'yashevich M.A., Stepanov B.I. *Kolebaniya molekul* (Vibrations of Molecules) (Moscow: GITTL, 1949) Vol. 2.
33. Kutepov A.M. (Ed.) *Voda: struktura, sostoyanie, sol'vatatsiya* (Water: Structure, State and Solvation) (Moscow: Nauka, 2003).
34. Yamaguchi T., Chong S.-H., Hirata F. *J. Chem. Phys.*, **119**, 1021 (2003).
35. Yamaguchi T., Matsuoka T., Koda S. *J. Chem. Phys.*, **120**, 7590 (2004).
36. Chandler D. *Nature*, **445**, 831 (2007).
37. Willard A.P., Chandler D. *J. Phys. Chem. B*, **112**, 6187 (2008).